INEEL/CON-04-02498
PREPRINT

What Can Granular Media Teach Us About Deformation In Geothermal Systems?

S. L. Karner

June 25-29, 2004

40th U.S. Rock Mechanics Symposium (ALASKA ROCKS 2005)

ARMA/USRMS 05-797

What can granular media teach us about deformation in geothermal systems?

Karner, S.L.
Idaho National Laboratory, PO Box 1625, Mailstop 2107, Idaho Falls, ID, 83415

ABSTRACT: Experiments on granular media have significantly improved our understanding of deformation processes in porous rocks. Laboratory results have lead to fundamental theoretical developments (such as poroelasticity, or rate and state-variable friction) that have found widespread application. This paper presents results from laboratory experiments that help constrain these theories. Data from triaxial deformation experiments on quartz sand aggregates are used to illustrate stress-dependent behavior of poroelastic parameters (e.g. the Biot-Willis and Skempton coefficients). Calculations for these coefficients show systematic variations as effective stress increases, in a manner consistent with measured compressibilities of the aggregate. Data from shear experiments show that frictional strength varies systematically with time and temperature. At temperatures below 450 ^{o}C, shear zones exhibit greater cohesive strengths as the time of stationary contact increases (hence, positive healing rates). For conditions exceeding 450 ^{o}C, shear zone strength is seen to decrease with contact time (negative healing rates). The results from both volumetric compaction and frictional shear experiments are well described by poroelasticity as well as rate and state-variable friction. The combination of these constitutive relations may provide a powerful tool that can be used in numerical models that couple thermal, mechanical, hydraulic, and temporal processes – as occur in geothermal systems.

1. INTRODUCTION

Both crystalline and sedimentary rocks permit the study of deformation processes such as brittle failure, inter- and intra-crystalline plasticity, fluid-rock interactions, and in-situ phase alterations. Yet, it is with clastic rocks that we are best able to study these processes together with the effects of consolidation, compaction, storage capacity, and fluid transport. Historically, studies of granular media have helped us understand the role of effective stress on deformation, the influence of consolidation and distortional stress on failure strength and yield behavior (i.e. critical state models), the characteristics of frictional shear, the time-dependent variations of material strength, the evolution of porosity and its relationship to permeability - just to name a few. These processes are fundamental for studies of natural systems (e.g. sediment compaction, fault mechanics, crustal rheology) and a variety of geosystems for which rock mechanics finds application (e.g. mining industry, hydrocarbon industry, water resources, and geothermal fields).

While several mechanisms are likely to alter petrophysical properties, it is important to note that processes associated with mechanical deformation of granular media are readily applicable to a variety of components in geothermal systems – such as proppants, clastic reservoirs, and fracture properties. Results from deformation experiments on granular media can be directly applied to clastic reservoirs and fracture proppants in order to estimate static strength characteristics, material properties, and geotechnical constants. Also, the temporal evolution of petrophysical properties of these materials can be investigated from laboratory studies of compaction creep and frictional shear in granular media. Yet, laboratory tests routinely indicate that deformation in granular media share many characteristics with deformation processes in crystalline rocks (e.g. frictional behavior) and fractured media (e.g. poroelastic behavior, fluid

transport properties). As such, those concepts derived from studies of granular media are deserving of consideration when the strength and fluid transport properties of fractures and shear zones are being analyzed.

Here, I report on laboratory results of deformation in granular media that have relevance for resource development in geothermal systems. The results highlight key topics currently associated with research activities in geothermal fields – such as poroelasticity theory, the strength properties of fractured reservoirs and granular proppants, the temporal evolution of fault strength and fracture propagation coupled with fluid transport properties, and the role of hydrothermal fluids on rock strength.

2. POROMECHANICS

2.1. Relevance to geothermal systems

A fundamental connection between fracture networks and granular media is that each contain a volumetric fraction of void space (porosity) embedded in a solid medium (see Fig. 1). At the modest pressures and temperatures of the shallow crust, the solid component (rock) accommodates deformation via a combination of elastic and brittle mechanisms that act to change the total pore volume. If fluids are present in the void space, then pore pressure and/or fluid transport properties of the rock may change with the evolving pore network. Any resulting changes in pore pressure may then perturb the stress state of the rock – an aspect that was documented by early work on granular media [e.g. 1-6]. It is this feedback between applied stress, deformation of the solid, volume change of the void space, and evolution of pore fluid pressure that forms the basis of modern poroelasticity theory via the concept of effective pressure.

Poroelasticity theory has been successfully applied to studies of granular media [5, 7-10], borehole damage [11-12], fractured media [10, 13], and fault mechanics [14-16]. With the combination of all these features, studies of fluid flow and fracture generation in geothermal systems provide an ideal focus topic to which poroelasticity theory can be applied. While it is not the focus of this paper to completely describe poroelasticity theory, the mathematical coefficients of the theory will be considered in the context of recent laboratory data.

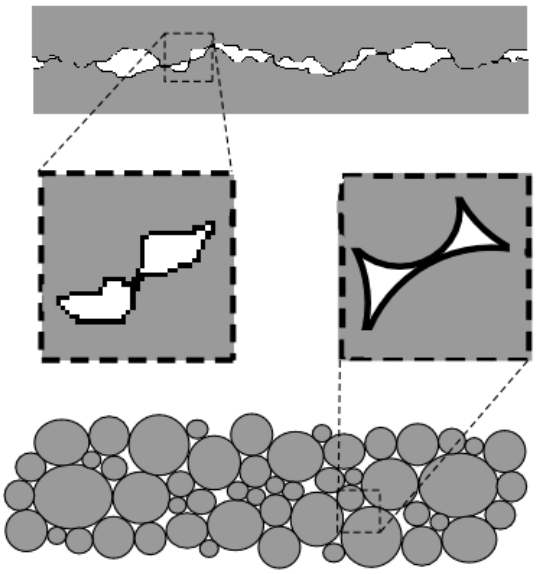

Fig. 1. Schematic comparison of void space (white) embedded in solid medium (gray) for a fracture (upper cartoon) and granular aggregate (lower cartoon). When the contacting grain boundaries and fracture walls are removed from the conceptual model, the embedded void space for each case look and behave remarkably similar to each other.

2.2. Poroelastic coefficients

Effective stress (σ_{ij}^{eff}) can be fully described by the relation [2, 17-19]:

$$-_{ij}^{eff} = -_{ij} - -p-_{ij} \quad (1)$$

where θ_{ij} is the full tensor of stress in the solid, θ_{ij} is the Kronecker delta, and p is the pressure of the fluid. The Biot-Willis effective stress coefficient (θ) describes how efficiently pore fluid can transfer pressure. The Biot-Willis coefficient can be readily defined in terms of the bulk modulus of the solid rock without pores (K_s) and the bulk modulus of the rock with pores (K_{bc}). However, the definition can be extended to relate to a variety of material properties (including porosity, θ) that are directly measured from experiments. If the confining pressure or pore pressure are independently varied (all the while maintaining the other constant - similar to drained experiments then the Biot-Willis coefficient can be expressed as) [19-21]:

$$\alpha = 1\,\alpha \left. K_{bc} \right/ K_s = \alpha K_{bc} \left/ K_{pc} \right. = \left. K_{bc} \right/ K_{bp} \quad (2)$$

The notation used here is that of [21], where the first subscript refers to the type of volume strain considered (b is bulk, p is pore) and the second subscript refers to the pressure change that induced the volume strain (c is confining pressure, p is pore fluid pressure).

A complete discussion of poroelastic deformation should account for the relationships between bulk volumetric strains that are observed for both undrained (θ_u) and drained materials (θ_d). If we consider the ratio of these volumetric strains then the following expressions can be derived [19, 21]:

$$\frac{-_u}{-_d} = \frac{K_{bc}}{K_u} = 1 - -B \qquad (3)$$

This introduces two new parameters: 1) K_u referred to as the undrained bulk modulus, and 2) a dimensionless geotechnical parameter, B, referred to as the Skempton coefficient [22]. The Skempton coefficient provides a coupling between a change in pore fluid pressure (θp) and the macroscopic deformation (in terms of applied mean stress, $\Delta\Delta$) of an undrained material via the relation [19]:

$$B = \frac{\sigma p}{\sigma\overline{\sigma}} = \frac{3\sigma p}{\sigma\mathbf{\sigma}\,\sigma_{ij}\sigma_{ij}} \qquad (4)$$

2.3. Laboratory observations

A fundamental problem for laboratory studies of poroelastic effects in fractured media is that the total fracture porosities are typically very low. Thus, it is difficult to experimentally measure the geotechnical parameters (θ and B) that are used in poroelasticity calculations. Furthermore, the void space formed by the fractures may not be an active part of an interconnected network at all times during deformation. Thus, fractured media may deform in a way that couples both drained and undrained characteristics. While these are important points in terms of proper modeling of fractured media, they highlight the difficulties in performing parametric studies of the poroelastic coefficients for fractures. Due to the large amount of interconnected pore space, laboratory experiments on granular media can remediate these problems and provide insightful information about poroelastic deformation.

It may be intuitively obvious that the poroelastic coefficients can vary according to differences in mineralogy and/or lithology (see Table 1). Further, it is reasonable to expect variations of these coefficients for a given rock type – such as for sandstones (Table 1) that exhibit a wide range for both the Biot-Willis coefficient (0.64-0.85) and Skempton's coefficient (0.5-0.88). However, it must be noted here that the values reported for a particular rock typically represent an average of many measurements taken over a narrow range of stress conditions. As such, any variations of these parameters that may occur for a given rock are concealed within the average.

Scalar values of the poroelastic parameters are often incorporated into numerical models of rock deformation. However, attempts to simulate dynamically evolving systems for which the stress state and/or rock properties are changing will necessitate the use of more complicated descriptions of the poroelastic parameters (for a tensorial description see [16]). Such an approach can be accomplished by utilizing those laboratory data that have revealed complex variations of the poroelastic parameters, such as seen for applied stress [23-24] and rock properties (e.g. anisotropy) [24-25].

Table 1. Poroelastic parameters of common porous rocks. Shown are laboratory measured values of porosity (θ), shear modulus (G, in GPa), bulk modulus (K, in GPa), the Biot-Willis coefficient (θ), and Skempton's coefficient (B). Values obtained from the References cited.

Rock	θ	G	K	θ	B	Ref
Charcoal granite	0.02	19	35	0.27	0.55	21
Westerly granite	0.01	15	25	0.47	0.85	21
Tennessee marble	0.02	24	40	0.19	0.51	21
Indiana limestone	0.13	12	31.2	0.69	0.46	22
Ruhr sandstone	0.02	13	13	0.65	0.88	21
Weber sandstone	0.06	12	13	0.64	0.73	21
Berea sandstone	0.19	6.0	8.0	0.79	0.62	21
Berea sandstone	0.19	5.6	6.6	0.78	0.75	22
Ohio sandstone	0.19	6.8	8.4	0.74	0.50	21
Pecos sandstone	0.20	5.9	6.7	0.83	0.61	21
Boise sandstone	0.26	4.2	4.6	0.85	0.50	21

2.4. Biot-Willis coefficient (θ)

Results from deformation experiments on initially unconsolidated St Peter quartz sand deformed under isotropic conditions show systematic changes in volume reduction (or compaction) with increasing stress that, when viewed in their entirety, clearly display a non-linear pressure dependence (Fig. 2a) [26]. For the tests shown in Fig. 2, the samples were deformed by monotonically increasing confining pressure at a constant rate while maintaining the pore pressure at a reference value of 12.5 MPa. Volumetric strains (cast in terms of porosity variations) were determined from the changes in fluid volume needed to maintain constant fluid pressure.

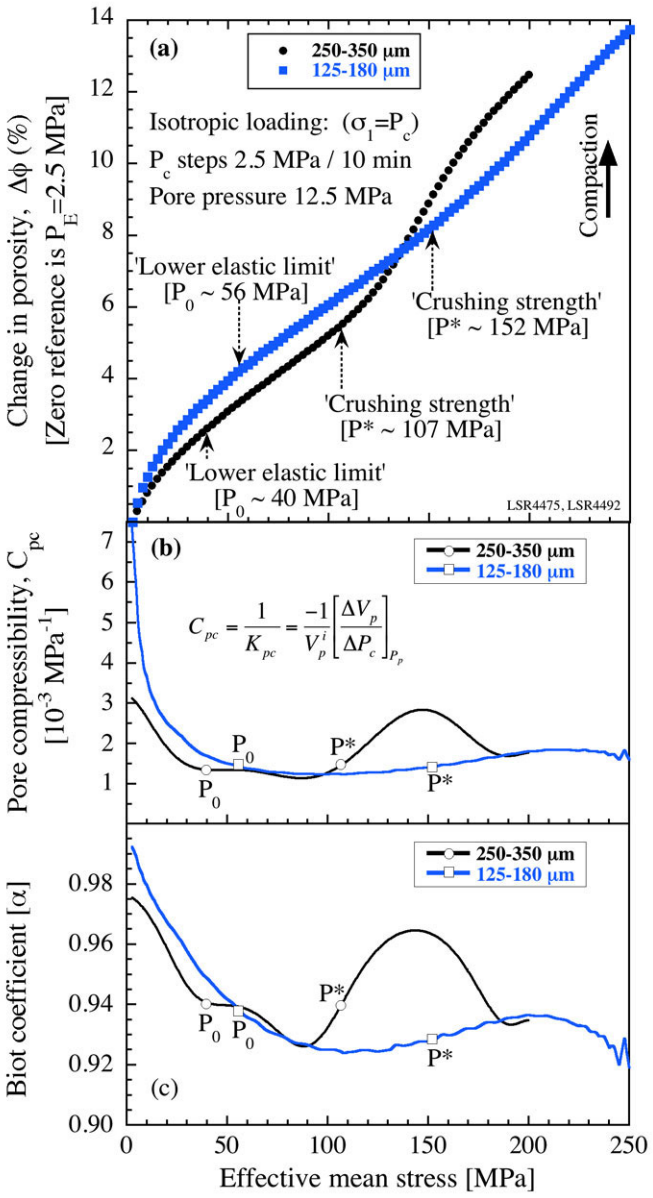

Fig. 2. Data from room-temperature isotropic deformation experiments on water-saturated St Peter quartz sand [26, 30]. Samples consisted of sieved fractions with mesh size range as shown. a). Sands were deformed by raising effective pressure 2.5 MPa every 10 minutes (pore pressure constant at 12.5 MPa). Volumetric strain (i.e. change in porosity) was directly determined from fluid volume expelled during compaction. b). Pore compressibility determined by using the equation shown (following the notation of [20]). For a given grain size fraction and effective stress, the experiment reproducibility is typically better than 5×10^{-4} MPa^{-1} [26]. c). Apparent Biot coefficient calculated from Eq. 5 using a bulk modulus (K_s) for quartz of 37.447 GPa [31], the pore compressibility calculated in (b), the change in porosity in (a), and the measured initial porosity (0.34 for 250-350 μm size fraction; 0.326 for 125-180 μm size fraction) [26]. The total range of θ for a given test (θ θ ~0.06) well exceeds experimental reproducibility (less than 0.01, determined from data in [26]).

The results are consistent with previous work [26-30] inasmuch as granular flow dominates at low stress (below the P_0 shown in Fig. 2), followed by quasi-elastic behavior at intermediate stresses (between P_0 and P* shown in Fig. 2), and post-yield cataclastic flow at high stresses (above P* shown in Fig. 2). The non-linear character of the stress-strain curve is due to inelastic deformation mechanisms that operate at low and high stresses [26, 30]. This non-linearity suggests that values of the 'apparent' poroelastic coefficient vary with loading stress.

As the stressing rate was fixed, volumetric strains can be directly converted to pore compressibility (see Fig. 2b) [20, 26]. When this is coupled with the measured porosity and the bulk modulus for quartz [31], an apparent Biot coefficient (θ) can be calculated via the relation (after rearranging Eq. 2):

$$\alpha = \alpha K_s \Big/ \left(\alpha K_s + K_{pc}\right) \qquad (5)$$

The calculated results clearly indicate that θ is not a constant quantity (Fig. 2c). That θ is near unity indicates that pore pressure has a significant influence on bulk strain [21], consistent with observations from soil mechanics [2]. It is important to note that the largest variations of θ occur at those parts of the stress-strain curve dominated by inelastic deformation mechanisms. Yet, for the quasi-elastic part of the loading curve the variation of θ is small, with levels that are well within the bounds provided by the relation $^{3\phi}/_{(2+\phi)} < \phi < 1.0$ [21].

The values for θ calculated for the deformed sand (Fig. 2) are greater than for any of the rocks listed in Table 1. This is due in large part to the unconsolidated nature of the material. However, rocks containing an abundance of fractures (as for stimulated geothermal reservoirs) may be quite compressible and could also have large values of θ [21]. Furthermore, fractured geothermal systems that are compressible will likely accommodate significant inelastic strains. As these strains are shown to alter the values of poroelastic parameters, numerical modeling of geothermal systems should attempt to utilize the constraints offered by these experiments.

2.5. Skempton's coefficient (B)

Another curious feature of these isotropic deformation experiments on quartz sand [26, 30] can be used to study other aspects of poroelastic deformation. While the sands for these experiments were stressed by step-wise increments in confining

pressure, apparatus limitations prevented pore pressure from being instantaneously changed as confining pressure was raised (Fig. 3). As such, the sands were essentially undrained for a brief interval after the increase in confining pressure (typically less than 30 seconds; see the Inset plot in Fig. 3a). As noted above for non-zero θ, any change in pore pressure will influence deformation (the converse also being true). As such, these tests provide an opportunity to explore the stress-dependent behavior of the Skempton coefficient (*B* in Eq. 4).

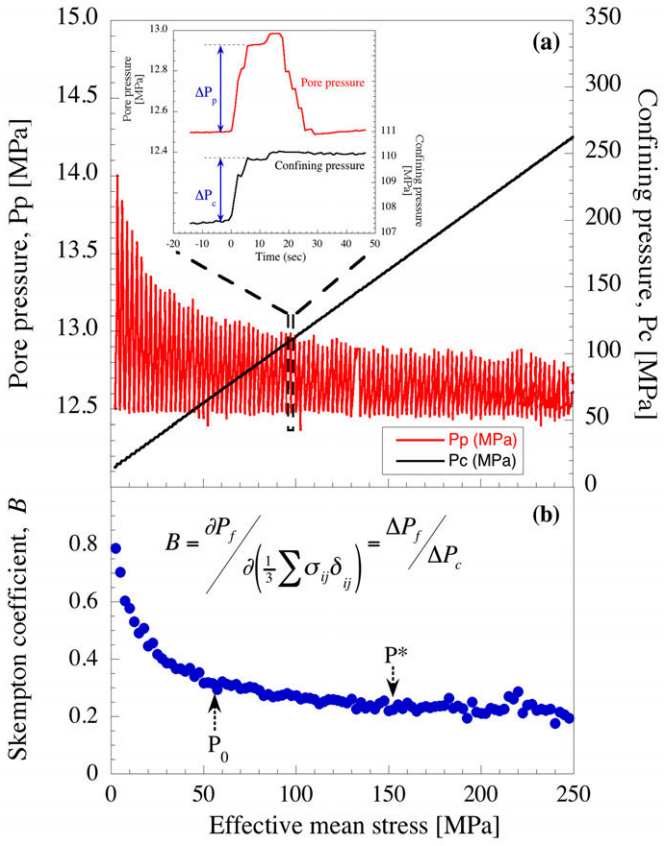

Fig. 3. Data from a room-temperature isotropic deformation experiment on water-saturated St Peter quartz sand [26, 30]. Experiment is the same as shown in Figure 2 with grain size fraction 125-180 μm. a). Confining and pore fluid pressures measured during the increase of effective pressure (θ_{eff} was raised 2.5 MPa every 10 minutes). Apparatus limitations were such that pore pressure could not immediately be maintained constant upon an step change in confining pressure. As such, a single step in confining pressure produced an increase in pore pressure (see Inset plot). Pore pressure was subsequently lowered to 12.5 MPa via an external pore fluid volumometer. The amplitude of the pore pressure response to each Pc step is seen to decrease at greater effective pressures. b). Skempton coefficient calculated for each step increase in θ_{eff} (using the modified form of Eq. 4 as shown in the plot). Data have been corrected for the compressibility of that volume of water contained in the apparatus system external to the sample.

The apparent Skempton coefficient has been calculated for each increment of stress (Fig. 3b). These experiments used a pore pressure generator situated a short distance away from the sample. Hence, as sample pore pressure rises with applied loading stress, a short-lived and negative pressure gradient develops between the sample and pressure generator. This gradient drives a small volume of fluid out of the sample and into the external portion of the pore fluid system, resulting in measured pore pressures that are less than expected for a truly closed sample [23]. This operational complexity can be corrected using known pressure-dependent compressibility of pore fluid (in this case, water) coupled with measured volumes of the apparatus pore fluid system and sample pore space. These corrected calculations are shown in Figure 3b.

For an undrained material, the amount of pore pressure rise due to a step in confining pressure is seen to be lower at greater effective pressures (Fig. 3a). This leads to calculated Skempton coefficients that systematically decrease as a function of effective pressure (Figure 3b). It is interesting to note that, when compared to the Biot coefficient (Fig. 2c), the Skempton coefficient seems less sensitive to the post-yield cataclastic deformation at loading stresses above P*. This apparent lack of sensitivity may be partly due to resolution issues (i.e. the 'signal' is within the 'noise' of the calculations of Skempton coefficient in Fig. 3b).

The relation between the Skempton coefficient and effective pressure shown for granular quartz sand (Fig. 3) can be qualitatively applied to fractures in geothermal systems. It has been noted that the deformation characteristics and permeability properties for contacting grains are similar to those for deforming asperities of a fracture [10, 32-34]. As such, the poroelastic characteristics of fractured media should behave in a similar manner to granular materials. In lieu of direct measurements on fractured rocks, the results from deformation tests on granular media can provide input for numerical models that predict the stress-dependent deformation behavior and fluid transport properties for geothermal systems. However, it is important to recall that these data provide little information about the temporal evolution of geomechanical and petrophysical properties. These properties must be adequately accounted for in order to properly sustain fluid flow over long intervals of time.

3. TIME-DEPENDENT CHARACTERISTICS

3.1. Strength evolution from recurrent seismicity

It is commonly assumed in studies of earthquake mechanics that the coseismic stress drop provides a measure of fault strength [e.g. 35-37]. Moment-magnitude data from seismic events occurring on the same fault patch indicate that stress drop increases with the time that elapses between consecutive events [38-39]. Furthermore, studies of trapped seismic waves within fault zones suggest that faults regain their strength in the months to years immediately following an earthquake [40]. As these observations span a large range of time scales, they should be considered when studying the temporal evolution of geothermal systems.

Laboratory experiments that involve bare rock faces sliding past each other have aided the development of fault mechanics and models of earthquake behavior (Fig. 4). These experiments inherently involve large shear strains, a component that may be comparatively insignificant for deformation in geothermal systems. However, the results from such experiments, coupled with similar experiments in granular media (as noted for glass beads [34]), can help provide a better understanding of strength evolution of fractures in geothermal systems.

Analysis of frictional data from stick-slip instabilities [33-34; see Fig 4] show that the stress drop values increase as a function of time between events (Fig. 4b). When coupled with observations of natural faults, these data imply that the cohesive strength of shear zones increases with time of stationary contact. It is often interpreted that shear zone strength evolves due to time-dependent deformation of asperities that act to increase the true area of contact [32, 41-43]. Predictions of time-dependent strength evolution in geothermal systems may be possible by studying repeating events from induced seismicity, in a manner similar to studies of natural faults [39].

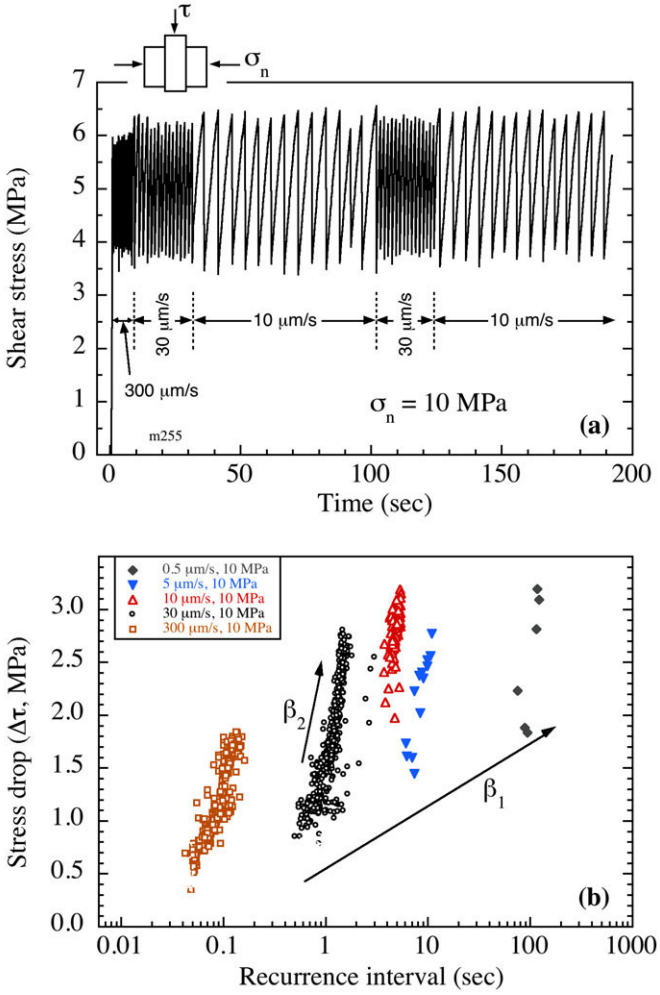

Fig. 4. Data from experiments on bare granite surfaces sliding past each other (modified from [33]). Normal stress across the sliding surfaces was held constant at 10 MPa. a). Typical shear stress data measured for a range of loading velocities imposed during double-direct shear of granite blocks (see Inset). The data display stick-slip instabilities, consistent with mechanical models of slip on seismically active faults and earthquake evolution. Note the variability in peak to peak amplitude of stress values around a sudden decrease in shear stress (stress drop). b). Stress drop values for the stick-slip events shown in (a), plotted as a function of time since the previous event (recurrence interval). Note the variability in stress drop values showing clear trends as a function of the imposed loading velocity (θ_1) and recurrence interval (for a given loading velocity, θ_2). The increase in stress drop with recurrence interval suggests that the surface regains strength as the time of stationary contact increases.

3.2. Restrengthening in granular media

In order to obtain a mechanistic understanding of fault restrengthening, frictional behavior can be studied via other experiments on shear zones that may or may not contain wear material (Fig. 5; for a review see [36]). Time-dependent friction effects have been extensively studied from slide-hold-slide tests (Figure 5). When the loadpoint velocity is set to zero for holds, friction decays owing to sample creep and subsequent stress relaxation (Fig. 5a). On reloading, friction increases to a peak value (a measure of the static frictional strength) and subsequently decays towards the pre-hold stable sliding level. The difference between the pre-hold friction level and the reload peak friction is taken as a measure of restrengthening or healing ($\theta\mu$).

Data from slide-hold-slide tests performed on layers of simulated fault gouge show that healing increases quasi-linearly with the logarithm of hold time

(Figures 5b). This is coupled with a similar hold time dependence of layer compaction (see [44] for details). As such, time-dependent frictional restrengthening has been interpreted to result from an increasing evolution in the number of grain to grain contacts (as layers undergo shear enhanced compaction). In this way, the results from shear tests on granular media are consistent with aging observed from friction tests on bare surfaces – inasmuch as the real area of contact increases with the time that the shear zone is held stationary.

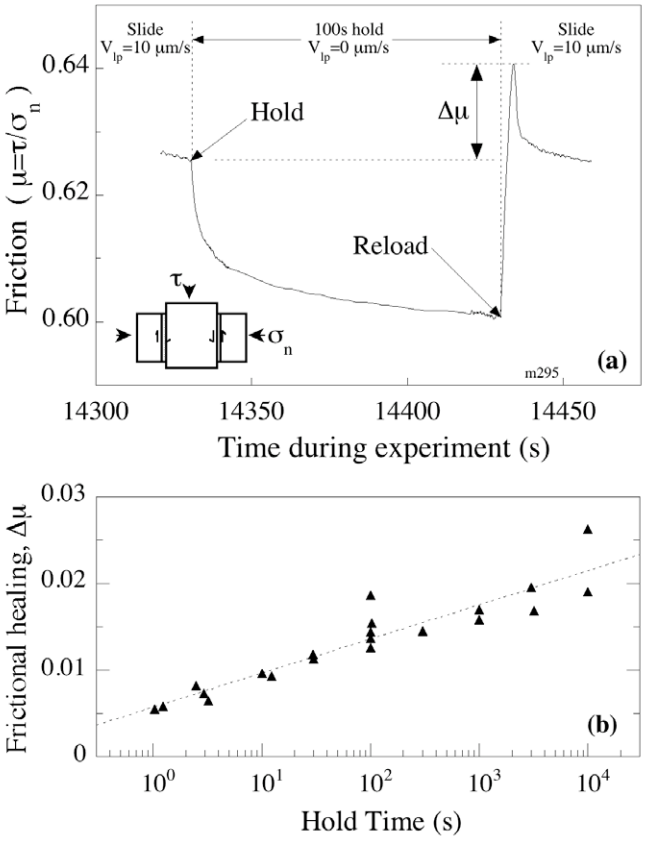

Fig. 5. Results from room-temperature slide-hold-slide tests in quartz sand (modified from [44]) performed in a double direct shear configuration (see Inset of Fig. 5a). a). Holds start when loading rate is set to zero. In holds, stress-relaxation occurs coupled with compaction of the layer (see [44] for details). Frictional restrengthening occurs on reloading ($\theta\mu$). b). The amount of restrengthening (healing) scales with the logarithm of hold time ($\theta\mu \sim 0.0052$ per decade change in time).

3.3. Rate and state friction constitutive relations

One outcome of laboratory friction studies has been the development of constitutive relations that describe friction evolution in terms of loading rate and the state of the shear zone. Of the friction relations that have been proposed, the rate- and state-dependent friction relations have been most frequently applied to analysis of rock friction data and to modeling of fault behavior [45-50], and are receiving the attention of researchers from other disciplines [e.g. 51-53]. These relations describe frictional sliding in terms of time-dependent evolution of contact strength or in terms of the slip necessary to alter frictional strength.

The general form of the rate and state variable constitutive relations describe shear stress (θ) in terms of external parameters such as normal stress, θ_n, and shear velocity, V, and internal variables that define the state of the sliding surface (θ_i):

$$\tau = f(\tau_n, V, \tau_i) \tag{6}$$

Evolution of the state of the sliding surface is given by an expression that describes how the state evolves with time towards a steady-state condition:

$$\frac{d\sigma_i}{dt} = g(\sigma_n, V, \sigma_i) \tag{7}$$

The two most widely used friction relations are: 1) the time-dependent (or slowness) law which I refer to as the Dieterich law, and 2) the slip-dependent law which I refer to as the Ruina law. These relations are similar in that they describe time and velocity dependence of friction (μ) by the relation:

$$\frac{\tau}{\tau_n} = \mu = \mu_0 + a \ln\left(\frac{V}{V_0}\right) + b \ln\left(\frac{V_0 \theta}{D_c}\right) \tag{8}$$

Here μ_0 represents steady-state friction for slip at a reference velocity, V_0, where V is the sliding velocity, D_c is a critical slip distance, θ is a state variable, and and b are scaling constants. However, the similarity between these relations does not extend to their description of evolution of the state variable. The Dieterich evolution law [45]

$$\frac{d\theta}{dt} = 1 - \left(\frac{V\theta}{D_c}\right) \tag{9a}$$

permits state evolution for frictional surfaces held in true stationary contact (V=0), whereas the Ruina evolution law [46]

$$\frac{d\theta}{dt} = -\left(\frac{V\theta}{D_c}\right) \ln\left(\frac{V\theta}{D_c}\right) \tag{9b}$$

requires some finite slip for the state to evolve. In applying these relations to laboratory data, equations 8-9 must be coupled with a relation describing elastic interaction with the loading apparatus: $d\mu/dt = k\,(V_L - V)$, where V_L is the loading velocity prior to a hold, and k is a measure of apparatus stiffness.

The Dieterich and Ruina laws are capable of describing a variety of friction observations from laboratory experiments, despite their different descriptions of state evolution. Several studies have shown that friction may evolve in a more complex manner than described by existing constitutive relations, such as for large variations in normal stress [54-55], or large changes in shear stress [44, 56]. Yet, the widespread applicability of the rate- and state-dependent friction relations make them a potentially valuable tool for modeling the strength evolution of fractures in geothermal systems.

3.4. Hydrothermal restrengthening rates

The discussions above highlight important aspects of geomechanical properties that can be studied from laboratory experiments. However, the results described above were all obtained from room-temperature tests and, therefore, may not provide a complete description for strength evolution in geothermal systems. Chemical reaction rates are typically too slow to explore the petrophysical and geomechanical evolution of fractures from hydrothermal laboratory experiments. Reaction rates can be enhanced if the fluid-rock surface area is increased. Thus, the large surface area of pore space in granular aggregates make them ideal materials to study the temporal evolution of rock properties at laboratory hydrothermal conditions.

It is commonly assumed that the extent of lithification in granular media increases with temperature and time. It is also assumed that lithification generally acts to increase the strength of a granular media. Indeed, the peak strength of water-saturated granular quartz powder (simulating fault gouge) does vary systematically with both temperature and time [57]. The peak strength of quartz gouge increases quasi-linearly with temperature (to 800°C). Yet, the temporal evolution of strength does not appear to be as straightforward.

Hydrothermal shear experiments can be used to constrain restrengthening models. Previous works have reported results from layers of powdered quartz subjected to slide-hold-slide tests performed at a range of temperatures [57-58]. The rate and state friction parameters (a, b, D_c from the friction constitutive relation shown in Eq. 8) were determined from data inversion using a Levenberg-Marquardt method (Fig. 6a) and the values from [57-58] are shown in Table 2. These parameters are important for friction analyses as they help constrain fault rupture models and slip patch source properties. Of particular note here is that the difference between the two friction coefficients (i.e. a and b from Eq. 8) can be compared to previous results used to determine frictional stability ([59], see Fig. 6b). Negative values of (a-b) indicate that a material is prone to seismic instability (velocity-weakening, between 50-350 °C in Fig. 6b) and that materials with positive values are always stable.

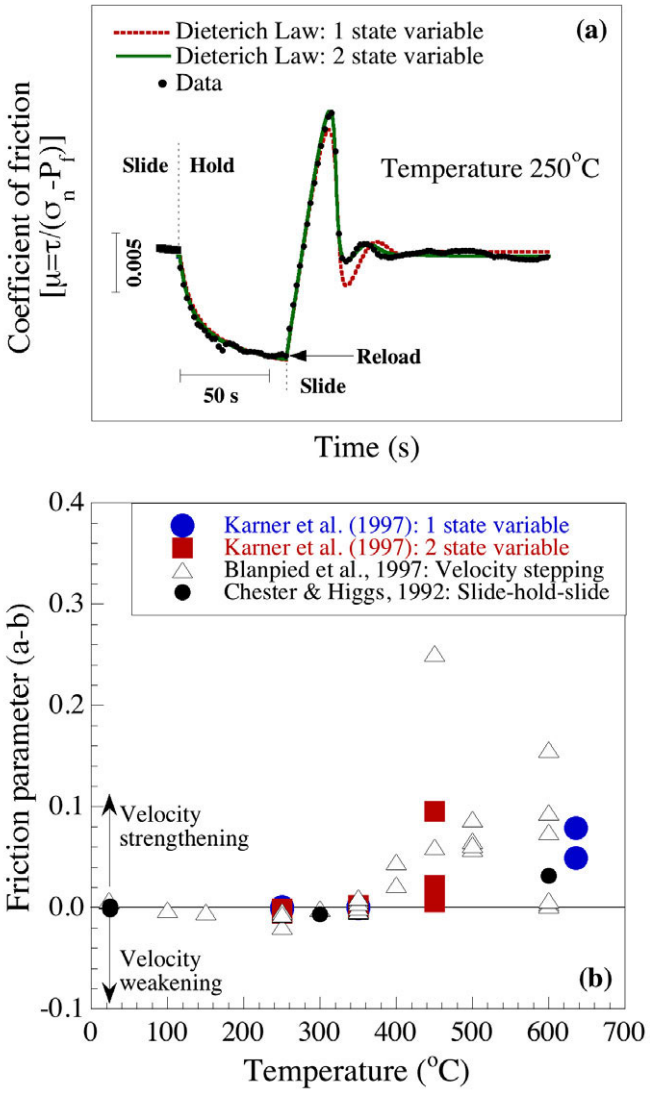

Fig. 6. Results from slide-hold-slide tests in layers of powdered quartz sand [44] performed in a double direct shear apparatus (Fig. 5a). a). The rate and state friction parameters (a, b, D_c in Eq. 8) were obtained from inversion of experiment data. For tests at a given temperature, the results from inversions using the Dieterich formulation were averaged and these are shown in Table 2. b). The difference between the friction parameters a and b are used to identify the conditions at which frictional instability may occur. Stability analyses of the hydrothermal slide-hold-slide tests presented here (for quartz powder layers) are consistent with both previous work on granite [59] and quartz sand [47].

Table 2. Rate and state friction parameters derived from numerical inversion of hydrothermal experiments on quartz powder layers [57-58]. Except for the highest temperature, inversions were performed using a two state-variable Dieterich model with the associated parameters indicated by subscripts.

Temperature	a	b_1	Dc_1 (μm)	b_1	$Dc_2(\mu m)$
250 °C	0.006	0.005	6.5	0.003	647.7
350 °C	0.005	0.005	4.4	-0.002	32.6
450 °C	0.052	0.003	3.3	-0.034	5845.8
600, 636 °C	0.016	-0.048	324.1	--	--

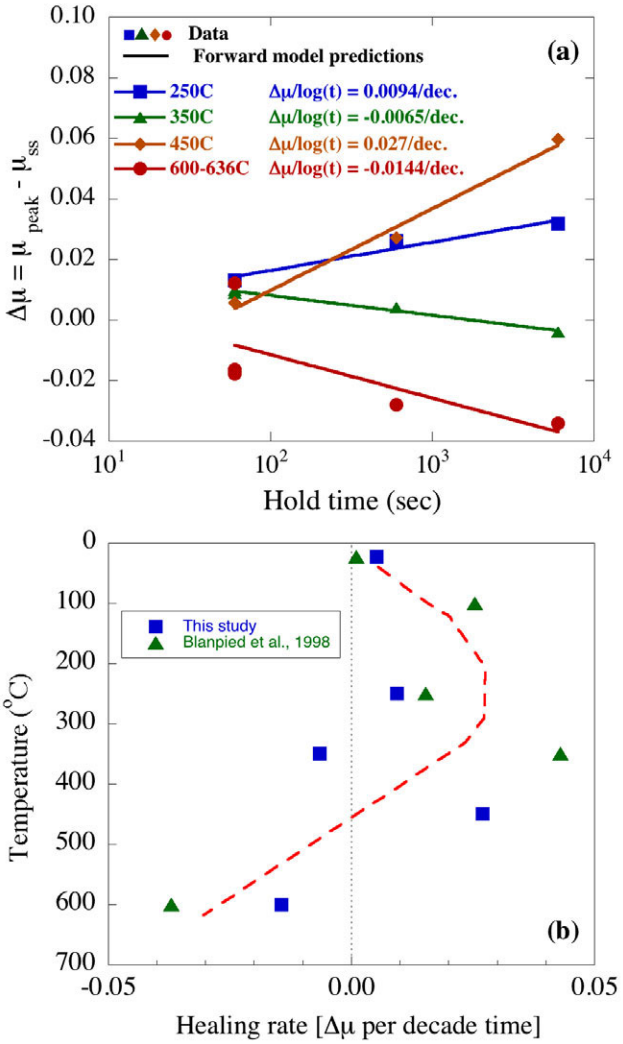

Fig. 7. Predictions of fault healing compared to the slide-hold-slide data shown previously in Figs. 5-6. a). Data for layers of quartz powder are well matched by the numerical predictions using the parameters shown in Table 2. b). The healing predictions shown in (a) are coupled with room-temperature healing data for quartz gouge (Fig. 5) and healing predicted from friction parameters derived for shear of granitic gouge [61]. Temperature is plotted as the vertical axis as a proxy for depth within the crust. The compilation of data indicate that healing rates vary as a function of temperature (or depth) with a transition to negative healing rates at very high temperatures (>500 °C). These results indicate that fractures in geothermal systems (T<350 °C) will tend to regain strength with time.

The friction parameters obtained from data inversion can also be used in forward models using the Dieterich friction evolution law (Eqs. 8-9a) to predict hydrothermal healing rates (see Fig. 7). The calculations provide a reasonable match to the observed data and indicate that healing rates vary with temperature (Fig. 7a). Furthermore, the results suggest that healing rates systematically decrease with increasing temperature, possibly due to thermally activated processes that enhance creep within the shear zone.

While the thermal conditions for these tests exceed those typically observed in geothermal systems, these laboratory results illustrate that temporal evolution of fracture strength can vary significantly with temperature. For typical geothermal fields (i.e. T<350 °C), the laboratory results also indicate that fractures embedded in silicate rocks (e.g. granites) will be conditionally unstable (velocity-weakening part of Fig. 6b) and display positive restrengthening rates with time (Fig. 7). When coupled with moment tensor analyses derived from induced seismicity, the laboratory results offer mechanistic interpretations that may enable predictive modeling of strength evolution and propagation of fractures. These aspects are fundamentally important when fracture networks in geothermal fields are expected to be sustained for a considerable amount of time.

4. RATE AND STATE POROELASTICITY: A POSSIBLE DIRECTION FORWARD?

Geothermal resources inherently involve a complex interplay between thermal conditions, mechanical properties, fluid-rock interactions, and time. If development of these resources is to be successful, then mechanistic and numerical models need to be built in such a way that they incorporate these coupled processes. These models must necessarily be constrained by theoretical and laboratory work so as to provide meaningful predictions. To this end, the well-constrained theories of poroelasticity (or, in extended form, thermo-poroelasicity) and rate and state friction can be used simultaneously to help understand geothermal systems.

Connections between the properties of porous media and rate and state friction relations have been previously noted [49-50]. Here, porosity evolution in a sheared granular medium can be described in terms of the rate of deformation and the state of the shear zone [after 49]:

$$\phi = \phi_0 + c \ln\left(\frac{V_0}{D_c}\right) \quad (10)$$

where θ_0 is a reference porosity, c is a dilatancy coefficient, and the variables V_0, θ, and D_c are as described previously (in Eq. 8). The state of the shearing material (θ) evolves according to the time or slip dependent forms given earlier (Eq. 9). Simulations of porosity evolution in a sheared granular material were found to compare reasonably well to laboratory data [49]. Additionally, recent work highlights several key points of similarity between the friction constitutive relations and conceptual models that have evolved from soil mechanics [60]. These results suggest that the friction relations can be extended to describe deformation in granular volume rather than the two dimensional limitations provided by frictional shear.

Together these works suggest that poroelasticity and rate and state friction are linked via their separate descriptions of porosity. I postulate here that these seemingly independent theories may be coupled to provide a more complete description of deformation in porous media. The rate- and state-dependent porosity expression (Eq. 10) can be incorporated into the description of the Biot-Willis coefficient (Eq. 5) to yield:

$$\alpha = 1 + \frac{K_s}{K_{pc}} \Big/ \left[\phi_0 + c \ln\left(\frac{V_0}{D_c}\right)\right] \quad (11)$$

where the state variable (θ) varies according to either the time or strain dependent evolution relations (Eq. 9).

Equation 11 allows the temporal predictions offered by rate and state theory to complement the coupled thermal, hydraulic, and mechanical descriptions of thermo-poroelasticity. While this may be extremely valuable for studies of porous media, it remains to be seen whether such a coupled constitutive relation could hold up to rigorous theoretical analysis and tested by constraints provided by laboratory experiments. As such, this may provide a rich line of research for future studies.

5. SUMMARY

Observations of laboratory experiments on granular media have lead to the development of several theories that can be applied to any porous material. These theories describe fundamental properties of porosity and fluid transport as a function of stress, temperature, and time. Of these properties, the observations reported in this paper stem from laboratory experiments that explore compaction in quartz sands as well as frictional shear in granular layers and on bare rock surfaces. The key aspects are as follows:

- deformation in porous media can be described in terms of mechanical stresses and dimensionless poroelastic parameters;
- the primary poroelastic parameters (the Biot-Willis and Skempton coefficients) are not constant quantities, as their values vary with 1. composition, 2. material properties, and 3. the amplitude of loading stresses;
- the strength of frictional surfaces and shear zones are observed to increase with the amount of time that imposed strain rates are held constant (or quasi-constant);
- the temporal evolution of fracture (or shear zone) strength is well described by existing rate- and state-dependent friction theory.

The combination of these observations and the associated constitutive relations can help to completely describe the processes of stress-induced deformation together with the temporal evolution of strength. As such, these relationships are valuable for studies of geothermal resources which inherently involve the coupling of thermal, mechanical, hydraulic, and temporal processes.

ACKNOWLEDGEMENTS

This work was supported by the U.S. Department of Energy, Assistant Secretary for Energy Efficiency and Renewable Energy, Office of Geothermal Technology, under DOE Idaho Operations Office Contract DE-AC07-99ID13727, whose support is gratefully acknowledged. Parts of the laboratory results in Section 2 were supported by the Office of Basic Energy Sciences, Division of Chemical Sciences, Geosciences, and Biosciences, Department of Energy, under Grant DE-FG03-ER14887. I thank Mike Shook and Stephen Novascone for their constructive reviews of this paper. I also thank Fred Chester, Judi Chester, Andreas Kronenberg and Chris Marone for guiding my thoughts at key points in time.

REFERENCES

1. Hertz, H., 1881. Ueber die Berührung fester elastischer Körper. *J. Reine Angew. Math.*, 92: 156– 171.
2. Terzaghi, C., 1925. Principles of soil mechanics: II. Compressive strength of clay. *Eng. News-Rec.*, 95: 796– 800.
3. Timoshenko, S., 1934. *Theory of Elasticity*. 1st Ed. New York: McGraw-Hill, 416 pp.
4. Graton, L.C., and H.J. Fraser, 1935. Systematic packing of spheres — with particular relation to porosity and permeability. *J. Geol.*, 43: 785– 909.
5. Biot, M.A., 1941. General theory of three-dimensional consolidation. *J. Appl. Phys.*, 12: 155–164.
6. Love, A.E.H., 1944. *A Treatise on the Mathematical Theory of Elasticity*. 4th Ed. New York: Dover Publ., 643 pp.
7. Mindlin, R.D., and H. Deresiewicz, 1953. Elastic spheres in contact under varying oblique forces. *J. Appl. Math.*, 75: 327– 344.
8. Geertsma, J., 1966. Problems of rock mechanics in petroleum production engineering, In *Proceedings of the 1st International Society of Rock Mechanics Congress*, v. 1, pp. 585-594, Lisbon.
9. Biot, M.A., 1973. Nonlinear and semilinear rheology of porous solids. *J. Geophys. Res.*, 78: 4924–4937.
10. Gangi, A.F., 1978. Variation of whole and fractured porous rock permeability with confining pressure. *Int. J. Rock Mech. Min. Sci. Geomech. Abstr.*, 15: 249-257.
11. Haimson, B.C. and C. Fairhurst, 1966. Hydraulic fracturing in porous-permeable materials. *J. Pet. Technol.*, 21: 811-817.
12. Abou-Sayed, A.S., C.E. Brechtel, and R.J. Clifton, 1978. In-situ stress determination by hydrofracturing: A fracture mechanics approach. *J. Geophys. Res.,* 83: 2851-2862.
13. Rice, J.R., and M.P. Cleary, 1976. Some basic stress diffusion solutions for fluid-saturated elastic porous media with compressible constituents. *Rev. Geophys. Space Phys.*, 14: 227-241.
14. Roeloffs, E.A., 1996. Poroelastic techniques in the study of earthquake-related hydrologic phenomena. *Advances in Geophysics*, 37: 135-195.
15. Parsons, T., R.S. Stein, R.W. Simpson, and P.A. Reasenberg, 1999. Stress sensitivity of fault seismicity: A comparison between limited-offset oblique and major strike-slip faults. *J. Geophys. Res.,* 104: 20,183-20,202.
16. Cocco, M., and J.R. Rice, 2002. Pore pressure and poroelasticity in Coulomb analysis of earthquake interactions. *J. Geophys. Res.*, 107 (No. B2), doi: 10.1029/2000JB000138 .
17. Biot, M.A., and D.G. Willis, 1957. The elastic coefficients of the theory of consolidation, *J. Appl. Mech., Trans. ASME*. 79: 596-601.
18. Guéguen, Y., and V. Palciauskas, 1994. *Introduction to the Physics of Rocks*. Princeton, NJ: Princeton University Press, 294 pp.
19. Wang, H.F., 2000. *Theory of Linear Poroelasticity with Applications to Geomechanics and Hydrogeology*. Princeton, NJ: Princeton University Press, 287 pp.
20. Zimmerman, R.W., 1991. *Compressibility of Sandstones*. New York: Elsevier, 173 pp.
21. Zimmerman, R.W., 2000. Coupling in poroelasticity and thermoelasticity. *Int. J. Rock Mech.*, 37: 79-87.
22. Hart, D.J., and H.F. Wang, 1999. Pore pressure and confining stress dependence of poroelastic linear compressibilities and Skempton's B coefficient for Berea sandstone. In *Proceedings of the 37th U.S. Rock Mechanics Symposium*, eds. B. Amadei, R.L. Kranz, G.A. Scott, and P.H. Smeallie, 365-371. Rotterdam: Balkema
23. Fredrich, J.T., and B. Evans, 1992. Strength recovery along simulated faults by solution transfer processes. In *Proceedings of the 33rd National Rock Mechanics Symposium*, eds. J.R. Tillerson and W. Wawersik, 121-130, Rotterdam: Balkema.
24. Lockner, D.A, and S.A. Stanchits, 2002. Undrained poroelastic response of sandstones to deviatoric stress change. *J. Geophys. Res.*, 107 (No. B12), 2353, doi: 10.1029/2001JB001460.
25. Lockner, D.A., and N.M. Beeler, 2003. Stress-induced anisotropic poroelasticity response in sandstone. *Electronic Proceedings of the 16th ASCE Engineering Mechanics Conference*, Seattle, 16-18 July 2003.
26. Karner, S.L., F.M. Chester, A.K. Kronenberg, and J.S. Chester, 2003. Subcritical compaction and yielding of granular quartz sand. *Tectonophys.*, 377 (3/4), 357-381.
27. Zhang, J., T-f. Wong, and D.M. Davis, 1990. Micro-mechanics of pressure-induced grain crushing in porous rocks. *J. Geophys. Res.*, 95, 341-352.
28. Wong, T-f., C. David, and W. Zhu, 1997. The transition from brittle faulting to cataclastic flow in porous sandstones: Mechanical deformation. *J. Geophys. Res.*, 102, 3009-3025.
29. Baud, P., W. Zhu, and T-f. Wong, 2000. Failure mode and weakening effect of water on sandstone. *J. Geophys. Res.*, 105, 16371-16389.
30. Karner, S.L., J.S. Chester, F.M. Chester, A.K. Kronenberg, A. Hajash Jr, 2005. Laboratory deformation of granular quartz sand: Implications for the burial of clastic rocks. *AAPG Bulletin*, IN PRESS: 89 (5).
31. Carmichael, R. S., 1984. *CRC Handbook of Physical Properties of Rocks: Vol. III*. Boca Raton, FL: CRC Press, 340 pp.
32. Dieterich, J.H., 1972. Time dependent friction in rocks. *J. Geophys. Res.*, 77: 3691-3697.

33. Karner, S.L. and C. Marone, 2000. Effects of loading rate and normal stress on stress drop and stick-slip recurrence interval. In *A.G.U. Monograph 120: Geocompexity and the Physics of Earthquakes*, eds. J.B. Rundle, D.L. Turcotte, W. Klein, 187-198. Washington DC: American Geophysical Union.

34. Mair K., K.M. Frye and C. Marone, 2002. Influence of grain characteristics on the friction of granular shear zones. *J. Geophys. Res.*, 107 (No. 10), 2219, doi: 10.1029/2001JB000516.

35. Scholz, C.H., 1992. *The Mechanics of Earthquakes and Faulting*. New York : Cambridge University Press, 439 pp.

36. Marone, C., 1998. Laboratory derived friction laws and their application to seismic faulting. *Annu. Rev. Earth Planet. Sci.*, 26: 643-696.

37. Beeler, N.M., S.H. Hickman, and T.-f. Wong, 2001. Earthquake stress drop and laboratory-inferred interseismic strength recovery. *J. Geophys. Res.*, 106: 30701-30713.

38. Kanamori, H., and C.R. Allen, 1986. Earthquake repeat time and average stress drop. In *Earthquake Source Mechanics, AGU Geophys. Mono. Vol. 37*, eds. S. Das, J. Boatwright & C.H. Scholz, 227-236. Washington DC: American Geophysical Union.

39. Marone, C., J.E. Vidale, and W.L. Ellsworth, 1995. Fault healing inferred from time dependent variations in source properties of repeating earthquakes. *Geophys. Res. Lett.*, 22: 3095-3098.

40. Li, Y-g., , J.G. Vidale, K. Aki, F. Xu, and T. Burdette, 1998. Evidence of shallow fault zone strengthening after the 1992 M7.5 Landers, California, earthquake. *Science*, 279: 217-220.

41. Bowden, F.P., and D. Tabor, 1954. *The Friction and Lubrication of Solids: Parts I, II*. London : Oxford University Press.

42. Dieterich, J.H., 1978. Time dependent friction and the mechanics of stick-slip. *Pure Appl. Geophys.*, 116: 790-805.

43. Hickman, S.H., and B. Evans, 1992. Growth of grain contacts in halite by solution transfer: Implications for diagenesis, lithification, and strength recovery. In Fault Mechanica and Transport Properties of Rocks. eds. B. Evans and T.-f. Wong, 253-280. San Diego: Academic.

44. Karner, S.L., and C. Marone, 2001. Frictional restrengthening in simulated fault gouge: Effect of shear load perturbations. *J. Geophys. Res.*, 106: 19319-19337.

45. Dieterich, J.H., 1979. Modeling of rock friction: 1. Experimental results and constitutive equations. *J. Geophys. Res.*, 84: 2161-2168.

46. Ruina, A., 1983. Slip instability and state variable friction laws. *J. Geophys. Res.*, 88: 10359-10370.

47. Chester, F.M., and N.G. Higgs, 1992. Multimechanism friction constitutive model for ultrafine quartz gouge at hypocentral conditions. *J. Geophys. Res.*, 97: 1857-1870.

48. Perrin, G., J.R. Rice, and G. Zheng, 1995. Self-healing slip pulse on a frictional surface. *J. Mech. Phys. Solids*, 43: 1461-1495.

49. Segall, P., and J.R. Rice, 1995. Dilatancy, compaction, and slip instability of a fluid infiltrated fault. *J. Geophys. Res.*, 100: 22155-22171.

50. Sleep, N.H., 1995. Ductile creep, compaction, and rate and state dependent friction within major fault zones. *J. Geophys. Res.*, 100: 13065-13080.

51. Géminard, J.-C., W. Losert, and J.P. Gollub, 1999. Frictional mechanics of wet granular material. *Phys. Rev. E*, 59: 5881-5890.

52. Berthoud, P., T. Baumberger, C. G'Sell, and J.-M. Hiver, 1999. Physical analysis of the state- and rate-dependent friction law: I. Static friction. *Phys. Rev. B*, 59: 14313-14327.

53. Baumberger, T., P. Berthoud, and C. Caroli, 1999. Physical analysis of the state- and rate-dependent friction law: II. Dynamic friction. *Phys. Rev. B*, 60: 3928-3939.

54. Linker, M.F., and J.H. Dieterich, 1992. Effects of variable normal stress on rock friction: Observations and constitutive equations, *J. Geophys. Res.*, 97: 4923-4940.

55. Richardson, E., and C. Marone, 1999. Effects of normal stress vibrations on frictional healing, *J. Geophys. Res.*, 104: 28859-28878.

56. Nakatani, M., 1998. A new mechanism of slip-weakening and strength recovery of friction associated with the mechanical consolidation of gouge. *J. Geophys. Res.*, 103: 27239-27256.

57. Karner, S.L., C. Marone, and B. Evans, 1997. Laboratory study of fault healing and lithification in simulated fault gouge under hydrothermal conditions. *Tectonophys*, 277: 41-55.

58. Karner, S.L. and C.J. Marone, 1997. Laboratory analysis and modeling of healing and lithification in simulated fault gouge. *Annales Geophysicae (Europ. Geophys. Soc. Symposia: Part I)*, v. 15 (supp. I): C-29.

59. Blanpied, M.L., D.A. Lockner, and J.D. Byerlee, 1995. Frictional slip of granite at hydrothermal conditions. *J. Geophys. Res.,* 100 : 13,045-13,064.

60. Karner, S.L., F.M. Chester, and J.S Chester, 2005. Towards a unified constitutive relation to describe granular deformation. *Earth Planet. Sci. Let.*, paper accepted pending revision.

61. Blanpied M.L., C.J. Marone D.A. Lockner, J.D. Byerlee and D.P. King, 1998. Quantitative measure of the variation in fault rheology due to fluid-rock interactions. *J. Geophys. Res.,* 103: 9691-9712.